A Scaling Law Governing Branching Morphogenesis in Neuronal Dendrites

Maijia Liao and Jonathon Howard[1]

Department of Molecular Biophysics & Biochemistry

Yale University

Key words: Allometry, microtubule transport, optimality, biological networks

[1]To whom correspondence should be addressed at joe.howard@yale.edu

Abstract (304 words)

Branched networks are ubiquitous in nature, ranging in size from watercourses and trees to cellular organelles and the cytoskeleton[1–5]. Often, the branch diameters change systematically throughout the network, with the proximal branches frequently thicker than the distal ones. This variation is usually interpreted as an adaptation to, or consequence of, the flow of materials and/or information through the network. To describe the changes in diameter over branch points, scaling or allometric relations of the form $d_{\mathrm{m}}^{p} = d_{\mathrm{d1}}^{p} + d_{\mathrm{d2}}^{p}$, have been proposed where d_{m} ($d_{\mathrm{d1}}, d_{\mathrm{d2}}$) is the mother (daughters) diameter and p is the exponent. Among the most well-known laws are da Vinci's rule for trees[6] ($p = 2$), Murray's law[7] for vascular and pulmonary systems ($p = 3$), and Rall's law[8] in the nervous system ($p = 3/2$). While scaling laws have a strong theoretical foundation, based on optimality arguments, and there is some experimental support[9,10], there is a dearth of critical tests and recent work in neurons, for example, finds sloppy morphology that defies optimization principles[11]. To test quantitatively scaling laws in the nervous system, we have established a new image-analysis method that allows us to resolve dendrite diameters down to 200 nm allowing us to measure the diameters of all branches in *Drosophila* Class IV dendritic arborization neurons, a model cell to study branching morphogenesis[12]. Unexpectedly, although the branch diameters vary systematically throughout the dendritic networks in these cells, they do not follow any of the known scaling laws. We propose a new scaling law governing dendritic morphology development. The law follows from two concepts: there is an incremental cross-sectional area needed to support each terminal branch, and there is a minimum branch diameter. The law is consistent with microtubule-based transport and tip extension in these cells. The new scaling law may also apply more generally to branching in other biological networks including the circulatory systems of animals[13,14] and plants[15,16].

Main text (1920 words including one table and four figure legends)

Drosophila Class IV neurons are highly branched sensory cells (Figure 1A-B) that serve as an excellent model system for studying dendrite morphogenesis[12]. Their arborizations grow to contain over 1000 branches, they can be marked with a GFP-tagged membrane protein expressed under a cell-specific promoter[17], they are located just under the cuticle, which allows imaging with high spatial and temporal resolution, and they are almost planar (Fig. 1B), which facilitates analysis and modeling.

To test scaling laws, accurate measurements of dendritic branch diameters are essential. Given the small sizes of the finest dendrites, conventional image analysis techniques based on thresholding techniques[9–11], cannot resolve the smallest diameters. To accurately measure dendrite diameters, we developed a super-resolution method that uses Monte-Carlo optimization to fit model images of Class IV dendrites to spinning-disk confocal images of dendrites whose surfaces were labeled with a membrane-associated fluorescent protein (Figure 1C). The model images are hollow cylinders with randomly distributed fluorophores convolved with the point spread function (PSF) of the confocal microscope. Even though the lateral resolution for the confocal microscope is ~200 nm ($\approx 0.5\lambda/\mathrm{NA}$, where $\mathrm{NA} = 1.2$ is the numerical aperture of the water immersion objective and $\lambda \approx 520$ nm is the emission wavelength), the method can resolve diameters <200 nm (Table 1), less than the diameters of the finest dendrites in these cells. We then applied our method to experimental images of dendrites. Fig. 1D shows that our simulated intensity profiles are close to the experimental ones and that the diameters of even the thinnest dendrites can be measured.

Table 1 Accuracies of diameter measurements.

True diameters of the model image (nm)	144	216	432	648	864
Measured diameters (Mean ± SD nm, $N = 18$ simulations)	140±25	222±16	422±24	659±22	880±19

The fluorophore density 1646/μm^2 was chosen based on estimations from the absolute intensity as well as from intensity fluctuations. Average over three cylinder orientations: 0.0, 0.5 and 1.0 rad relative to axial direction.

Before testing the scaling laws, we first confirmed that dendrite branches have well-defined diameters. We imaged one to three arbors of the dendritic trees of six fully-

developed third instar larvae (~132 hours after the egg was laid, which is defined as time 0). We measured diameters, defined in Figure 2A, at three positions along 306 branches from the six larvae, and plotted the normalized diameter against the normalized displacement along the branch, where zero displacement is towards the cell body (Fig. 2B, see Supplementary Information for details). The slope is -2.3%, which is small compared to the average reduction in diameter from the proximal mothers (18%) to the distal daughters (11%). Thus, the branch segments have approximately constant diameter, and the diameter changes primarily across branch nodes.

To test existing scaling laws, we fit the scaling equation presented in the abstract to the 253 branch points in the six cells from six 132-hr larvae that were used in Figure 2B. These branches sampled the full range of branch orders. Analysis of the experimental data reveals a large spread in the values of the exponent p (Fig. 2C). The mean of 7.23 does not support any of the aforementioned scaling laws. Furthermore, the wide range of exponents (SD = 8.8) is not consistent any specific scaling law. Alternative allometric relations are therefore required.

Class IV neurons come in a variety of shapes and possess dendritic trees that exhibit complex branching patterns. Among a wide range of allometric relations that we tested, we discovered a linear relationship between the leaf number, n, of a branch (the number of tips that the branch supports, Figure 3A) and the branch's cross-sectional area (Figure 3B): $\pi d^2/4 = \beta n + \pi d_0^2/4$, where β is the slope and the y-intercept is proportional to d_0^2, the square of the diameter of the terminal branch minus $4\beta/\pi$. Because the leaf number satisfies the simple allometric relation: $n_{\mathrm{m}} = n_{\mathrm{d1}} + n_{\mathrm{d2}}$ where n_{m} ($n_{\mathrm{d1}}, n_{\mathrm{d2}}$) are the leaf numbers of the mother (daughters), the linear relationship implies a new allometric scaling law: $d_{\mathrm{m}}^p + d_0^p = d_{\mathrm{d1}}^p + d_{\mathrm{d1}}^p$ (see Supporting Information for details). This provides a good fit to the experimental data (Figure 3C) and the exponent p is narrowly distributed with an average near two, corresponding to cross-sectional area (Fig. 3D). Thus, our new generalized scaling law with a minimum diameter provides a good fit to diameter scaling in Class IV dendrites.

Class IV neurons grow throughout larval development from a width of ~50 μm at 24 hrs to ~500 μm at 132 hrs (see Supporting Information). To complete the description of allometric scaling, we applied the postulated relation $d^p = \bar{\beta} n + d_0^p$ over all stages of

development. Figure 4A-C show that the scaling parameters are roughly constant throughout development. The average value over developmental time of the exponent p is 2.38 ± 0.80, (mean ± SD, 31 larvae) corresponding approximately to area scaling (Figure 4A). The average value over developmental time of the cross-sectional area per leaf is $1970 \pm 670\ \mathrm{nm}^2$ (±SD) (Figure 4B). The average value over developmental time of the terminal diameter ($d_1 = (d_0^p + \bar{\beta})^{1/p}$) is 237 $\pm$ 14 nm (±SD) (Figure 4C).

Scaling laws have been interpreted theoretically as optimal solutions to the transport of material or information. For example, the exponent $p = 3$ in Murray's law minimizes the work done by the heart or lungs to pump blood or air through the vascular or pulmonary systems, while keeping the volume of blood or air constant. The exponent $p = 3/2$ in Rall's law minimizes the propagation time of action potentials, assuming a constant density of channels (see Supporting Material and a related result in ref[18]).

We now offer a cell biological interpretation of the new scaling law. The increase in cross-sectional area ($p = 2$) with leaf number can be interpreted as a nutrient flux proportional to tip growth, which is proportional to the number of tips. Class IV neurons grow throughout development and the primary mechanism by which dendrite length increases is through tip extension (manuscript in preparation). This interpretation assumes that dendritic transport velocity is independent of dendrite diameter so that flux is proportional to cross-sectional area. The extra cross-sectional area per leaf of 2000 nm^2 is similar to the area occupied by one microtubule and a 30-nm vesicle carried along it by a motor protein (an ellipsoid with axes 35 nm and 70 nm). The interpretation is that each tip requires an addition microtubule to service it. A similar argument has been used to estimate the minimum diameter of axons[19].The minimum observed diameter of 230 nm may be bounded by the force required for dendrite extension. The minimum force, f, required to extend a tube of membrane with bending stiffness κ and diameter d is $f = 4\pi\kappa/d$ (ref[20]). For a stiffness of 40 pN/nm (ref[21]), this corresponds to $\cong$ 2 pN, which is similar to the force generated by a single growing microtubule[22] or a single microtubule-based motor[23]. The minimal diameter may also be limited by the kinetics of microtubule growth if the membrane must bend in order to allow additional tubulin dimers to be added to the microtubule end (see Supporting Information). In several ways, therefore, our new scaling law accords with microtubule-based transport. Thus, our analysis supports Cajal's

hypothesis that "all of the morphological features displayed by neurons appear to obey precise rules [e.g. scaling laws] that are accompanied by useful consequences [e.g. optimizing transport required for growth]"[24].

Our new scaling law may generalize to other systems. The pipe model for plants, which is equivalent to da Vinci's rule, posits that the amount of leaves is proportional to the cross-sectional area of soft (living) wood[15,16]. Including a minimum diameter, however, provides a better fit to some of the experimental data (Supplementary Information). Furthermore, Murray's law, which is difficult to test due to the large size of circulatory systems and their depth within the body, may be "improved" if a minimum diameter term is added: when it is, the spread in exponents[10] is reduced (Supplementary Information). Thus, scaling laws that consider vessels having a minimum diameter may apply generally to the branching in other biological networks.

Acknowledgements

We thank Xin Liang for initiating this project and members of the Howard laboratory for comments on an earlier draft. We benefited from discussions with Yuhai Tu (IBM Watson Laboratory, NY) during the execution of this work. This study was supported by NIH grant DP1 MH110065.

Figures

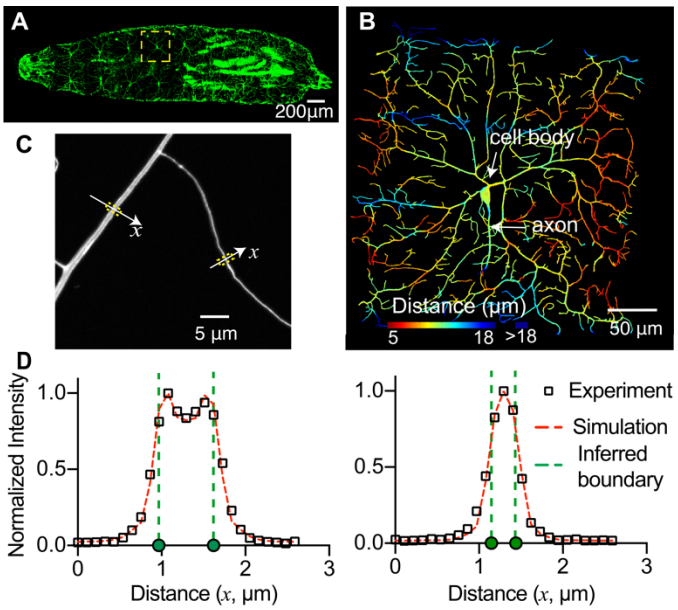

Fig. 1| Precise measurement of dendritic branch diameter. A Third instar larva expressing GFP in their class IV da neurons. The class IV ddaC neuron in abdominal segment 3 (A3) is boxed. Anterior is left. The A3 segment from which the cell in B is taken, is shown as dashed square. **B** Maximum projection image of ddaC neuron in A3 segment constructed from 76 stacks (separated by 0.2 µm) from a spinning disk confocal microscope (Nikon spinning disk, 50 µm pinholes, 40X water-immersion (WI) objective) of a 92 hr after egg lay larva from *Shi*^{ts1}*;;ppkCD4-tdGFP* fly. The distance of dendrites relative to the coverslip is color-coded. Note that the cells are mostly within a depth of ~12 µm, about 4% of their width. This dendritic tree has three arbors emerging from its cell body. **C** Maximum intensity projection images of a thick and a thin dendrite of a ~100-hr larvae expressing *Shi*^{ts1}*;;ppkCD4-tdGFP* from 60X WI objective with numerical aperture of 1.2. The yellow boxed regions with lateral width 1.1 µm indicate the part of dendrite where the intensity profile in **D** was obtained. **D** Intensity profiles of the middle section of the confocal stack for thick and thin dendrites in **C**. The inferred diameters are 657 nm and 292 nm as indicated by green dashed lines.

[one-column width: 89 mm = 3.5”]

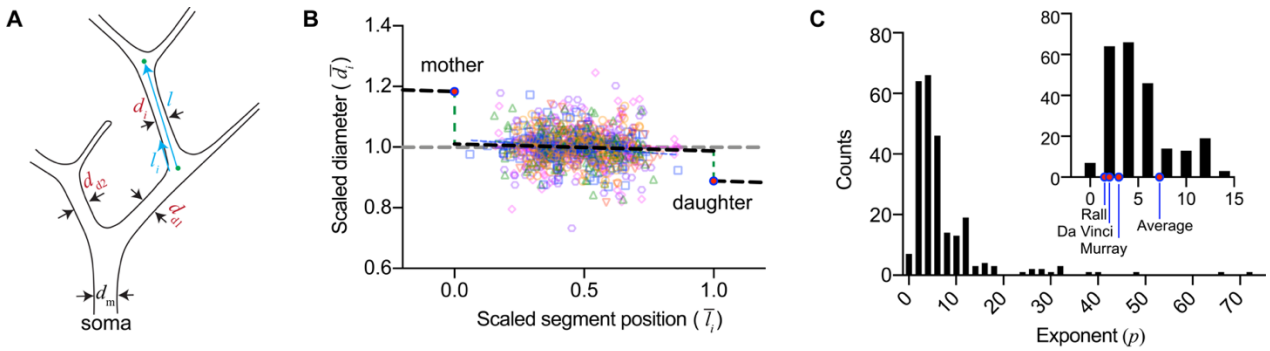

Fig. 2| Dendritic branch diameters do not obey known scaling laws. A Definitions of diameters. **B** Scaled diameters ($\bar{d}_i$: d_i to mean diameter of the branch) plotted against scaled segment position ($\bar{l}_i$: l_i to total length of the branch l). Two branches were selected for each branch order between 0-34 for 6 neurons from six 132-hr larvae. The number of diameter measurements from each neuron ranged from 90 to 204. Black dashed line represents the linear regression with slope -0.023 ± 0.013 ($\pm$ SEM, $P = 0.078$). The left and right magenta filled circles are the mean diameters of the mothers and the daughters. **C** The histogram shows the counts distribution of values of the exponent p fitted from for 253 neuron branch points from six 132-hr larvae. The average exponent is 7.2 and the standard deviation is 8.8. Inset shows an enlarged view with magenta filled circles indicating exponents predicted by the Rall, da Vinci and Murray scaling laws.

[two-column width: 183 mm = 7.2”]

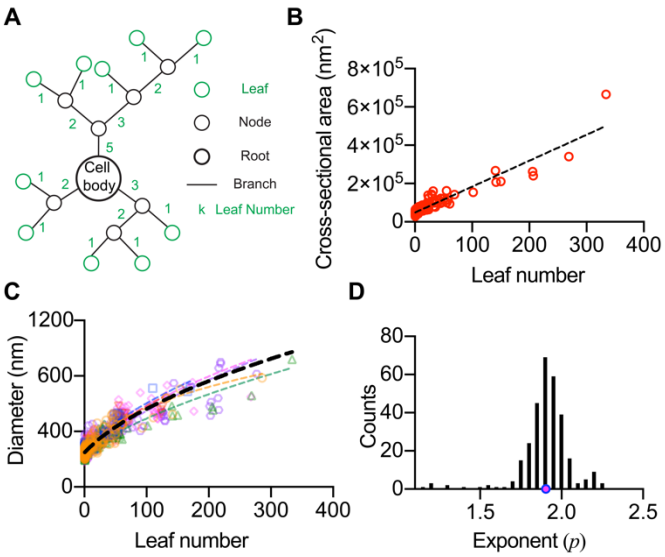

Fig. 3| A new scaling law for bifurcating dendrites. A Definition of the leaf number of a bifurcating tree. **B** Cross-sectional area vs. leaf number (one 132-hr larva). Black dashed line indicates linear regression with slope β $1.36 \pm 0.03 \times 10^3\ n\mathrm{m}^2$and y-intercept: $4.8\ \pm\ 0.1 \times 10^4\ n\mathrm{m}^2$. **C** Branch diameter vs. leaf number for six 132-hr larvae. Colored dashed curves stand for non-linear fittings $d^p\ = \bar{\beta} n + d_0^p$ for each neuron. Black dashed curve shows fitting for all data points, $p = 1.93 \pm 0.06$, $d_0 = 244 \pm 2$ nm (±SE, 1419 data points). **D** The histogram shows the counts distribution of values of the exponent p fitted from: $d_{\mathrm{m}}^p + d_0^2 = d_{\mathrm{d1}}^p + d_{\mathrm{d2}}^p$ for 303 neuron branch points from six 132-hr larvae. The average exponent value, denoted by magenta circle, is 1.90 ± 0.15 (±SD).

[one-column width: 89 mm = 3.5”]

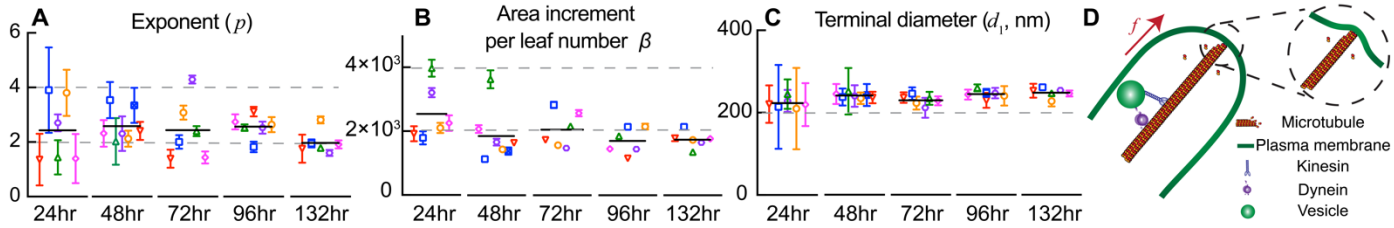

Fig.4 | New scaling law measured at different developmental stages and its physical interpretation. Scaling exponent p, (**A**), increment per leaf, β (**B**), and terminal diameter, d_1 (**C**), measured at different developmental stages. Symbols indicate means and vertical lines indicate SEs obtained from fits to six or seven individual cells at each stage of $d^p = \bar{\beta} n + d_0^p$. Black lines denote averages. **D** Scale drawing illustrating how essential components can be packed into the cross-section of an ellipsoid with axes 70nm and 35nm corresponding to incremental area per leaf (see text for details).
[two-column width: 183 mm = 7.2”]

References (24)

1. Bejan, A. & Zane, J. P. *Design in nature: How the constructal law governs evolution in biology, physics, technology, and social organizations*. (2013).

2. Ball, P. *Branches: Nature's patterns: a tapestry in three parts*. (2009).

3. Rinaldo, A., Rigon, R., Banavar, J. R., Maritan, A. & Rodriguez-Iturbe, I. Evolution and selection of river networks: Statics, dynamics, and complexity. *Proc National Acad Sci* **111**, 2417–2424 (2014).

4. Rafelski, S. M. *et al.* Mitochondrial network size scaling in budding yeast. *Science (New York, N.Y.)* **338**, 822–824 (2012).

5. Fletcher, D. A. & Mullins, R. D. Cell mechanics and the cytoskeleton. *Nature* **463**, 485–92 (2010).

6. Richter, J. P. *The notebooks of Leonardo da Vinci*. vol. 2 (1970).

7. Murray, C. D. The Physiological Principle of Minimum Work: I. The Vascular System and the Cost of Blood Volume. *Proc National Acad Sci* **12**, 207–214 (1926).

8. Rall, W. Branching dendritic trees and motoneuron membrane resistivity. *Experimental neurology* **1**, 491–527 (1959).

9. Zamir, M. & Medeiros, J. A. Arterial branching in man and monkey. *J Gen Physiology* **79**, 353–360 (1982).

10. Kassab, G. S. & Fung, Y.-C. B. The pattern of coronary arteriolar bifurcations and the uniform shear hypothesis. *Ann Biomed Eng* **23**, 13–20 (1995).

11. Otopalik, A. G. *et al.* Sloppy morphological tuning in identified neurons of the crustacean stomatogastric ganglion. *Elife* **6**, e22352 (2017).

12. Jan, Y.-N. & Jan, L. Y. Branching out: mechanisms of dendritic arborization. *Nat Rev Neurosci* **11**, 316–328 (2010).

13. LaBarbera, M. Principles of design of fluid transport systems in zoology. *Science* **249**, 992–1000 (1990).

14. Jr, J. T. D., Brown, B. G., Bolson, E. L. & Dodge, H. T. Lumen diameter of normal human coronary arteries. Influence of age, sex, anatomic variation, and left ventricular hypertrophy or dilation. *Circulation* **86**, 232–246 (1992).

15. Shinozaki, K., Yoda, K., Hozumi, K. & Kira, T. A quantitative analysis of plant form-the pipe model theory : I. basic analyses. *Jpn J Ecol* **14**, 97–105 (1964).

16. Lehnebach, R., Beyer, R., Letort, V. & Heuret, P. The pipe model theory half a century on: a review. *Ann Bot-london* **121**, 773–795 (2018).

17. Grueber, W. B. *et al.* Projections of Drosophila multidendritic neurons in the central nervous system: links with peripheral dendrite morphology. *Development* **134**, 55–64 (2007).

18. Wen, Q. & Chklovskii, D. B. A Cost–Benefit Analysis of Neuronal Morphology. *J Neurophysiol* **99**, 2320–2328 (2008).

19. Faisal, A. A., White, J. A. & Laughlin, S. B. Ion-Channel Noise Places Limits on the Miniaturization of the Brain's Wiring. *Curr Biol* **15**, 1143–1149 (2005).

20. Derényi, I., Jülicher, F. & Prost, J. Formation and Interaction of Membrane Tubes. *Phys Rev Lett* **88**, 238101 (2002).

21. Kamal, M. M., Mills, D., Grzybek, M. & Howard, J. Measurement of the membrane curvature preference of phospholipids reveals only weak coupling between lipid shape and leaflet curvature. *P Natl Acad Sci Usa* **106**, 22245–50 (2009).

22. Dogterom, M. & Yurke, B. Measurement of the Force-Velocity Relation for Growing Microtubules. *Science* **278**, 856–860 (1997).

23. Howard, J. Mechanics of motor proteins and the cytoskeleton. (2001).

24. Cajal, S. R. Histology of the nervous system of man and vertebrates. *History of Neuroscience (Oxford Univ Press, New York)* (1995).